

**Radiant star nanoparticle prodrugs for the treatment of  
intracellular alveolar infections**

Journal:	<i>Polymer Chemistry</i>
Manuscript ID	PY-ART-02-2018-000202.R2
Article Type:	Paper
Date Submitted by the Author:	22-Mar-2018
Complete List of Authors:	Das, Debobrato; University of Washington, Bioengineering Srinivasan, Selvi; University of Washington, BioEngineering Brown, Fiona; University of Washington, Bioengineering Su, Fang; University of Washington, BioEngineering Burrell, Anika; University of Washington, Biochemistry Kollman, Justin; University of Washington, Biochemistry Postma, Almar; CSIRO, Manufacturing Ratner, Daniel; University of Washington Department of Bioengineering Stayton, Patrick; University of Washington, Bioengineering Convertine, Anthony; University of Washington, Bioengineering



Journal Name

ARTICLE

## Radiant star nanoparticle prodrugs for the treatment of intracellular alveolar infections

D. Das,<sup>a</sup> S. Srinivasan,<sup>a</sup> F. D. Brown,<sup>a</sup> F. Y. Su, A. L. Burrell,<sup>b</sup> J. M. Kollman,<sup>b</sup> A. Postma,<sup>c</sup> D. M. Ratner,<sup>a</sup> P. S. Stayton\*, and A. J. Convertine<sup>a,\*</sup>

Received 00th January 20xx,  
Accepted 00th January 20xx

DOI: 10.1039/x0xx00000x

www.rsc.org/

Radiant star nanoparticle (RSN) prodrugs were synthesized in a two-step process by first homopolymerizing RAFT transmitters followed by copolymerization from the hyperbranched polymer core. Two trithiocarbonate-based transmitters were synthesized containing either alkyl ester or acetal groups linking the polymerizable methacrylate group to the chain transfer agent (CTA). RAFT polymerization from the homopolymerized transmitter cores yielded RSNs with linear polymer chains connected to hyperbranched cores. Hydrolysis studies conducted over a period of 30 days at 37 °C in acetate buffer showed that RSNs prepared from alkyl ester linked cores remained stable while acetal linked cores exhibited a progressive degradation into linear polymers over the same period. Macrophage targeting RSN prodrugs containing the antibiotic ciprofloxacin and receptor-targeting mannose residues were synthesized directly via RAFT polymerization of the prodrug and mannose monomers. Hydrolysis studies conducted in human serum showed that the RSNs released the covalently linked ciprofloxacin significantly faster than diblock copolymer micelles but moderately slower than soluble copolymers with comparable compositions. Flow cytometry showed substantially higher macrophage binding by the mannose-targeted RSNs while in vivo biocompatibility experiments showed no differences relative to phosphate buffer treated negative controls.

### A Introduction

Polymeric prodrugs are a strategy for overcoming the limitations typically associated with physically encapsulating drug delivery systems.<sup>1-4</sup> These prodrugs consist of therapeutic agents that have been covalently conjugated to a macromolecular scaffold via a hydrolytic or enzymatically degradable linkage. This strategy has been shown to substantially increase the solubility and stability of the parent drug while also enhancing drug circulation half-lives and reducing immunogenicity.<sup>5-8</sup> An attractive route for the synthesis of polymeric prodrugs is the direct reversible deactivation radical polymerization (RDRP) of therapeutic agents that have been reversibly modified with suitable vinyl functionality.<sup>9-20</sup> These polymerizable prodrug monomers (PPMs) allow for the facile incorporation of drug moieties into the final polymer at predetermined ratios without the need for additional conjugation and purification steps.

Recently, we reported the synthesis of polymeric prodrugs

using PPMs based on derivatives of the antibiotic ciprofloxacin.<sup>11</sup> Drug release studies conducted in human serum showed that the phenyl ester-linked antibiotic was cleaved from the polymer scaffold at higher rates relative to the aliphatic ester-linked drug. These differences in the relative antibiotic release rates were found to strongly influence the antimicrobial activity of the polymeric prodrugs with ciprofloxacin linked via phenyl esters showing significantly lower minimum inhibitory concentrations than the aliphatic ester linked prodrugs. Subsequent animal studies confirmed the therapeutic effectiveness of this system with the phenyl ester-linked polymeric prodrugs showing high cure efficiencies in completely lethal murine *Francisella tularensis* subsp. *novacida* pulmonary challenge models, while mice treated with free ciprofloxacin succumbed to the bacterial infection within a few days of exposure.<sup>21</sup>

Diblock copolymer-based prodrugs that self-assemble under physiological conditions to form nanoparticles are desirable from a drug delivery perspective, as they can contain the covalently linked prodrugs at a significant fraction of their total mass. These systems also typically show longer in vivo circulation times relative to analogous linear polymers and can provide preferential uptake in some cell populations, such as macrophages, because of their size and ability to display multivalent receptor-specific targeting ligands.<sup>22</sup> Despite these advantages, diblock copolymer based nanoparticles, where the covalently linked prodrugs are localized in the hydrophobic

<sup>a</sup> Molecular Engineering and Sciences Institute, department of BioEngineering, Box 355061, Seattle WA, 98195, USA. E-mail: aconv@uw.edu; Tel: +(206) 817 6011

<sup>b</sup> University of Washington; Department of Biochemistry

<sup>c</sup> The Commonwealth Scientific and Industrial Research Organization (CSIRO) Manufacturing, Bayview Avenue, Clayton, Victoria, 3168, Australia

core, typically show low rates of drug release.<sup>11,13</sup> Additionally, self-assembled structures such as micelles and liposomes can interact with serum proteins in vivo resulting in partial or complete disassociation of the constituent polymer or lipids.<sup>23</sup> Interaction of these structures with serum proteins can also cause them to be eliminated by the mononuclear phagocytic system or, in the case of encapsulation-based drug delivery, result in extraction of the physically bound drugs.<sup>24</sup>

The incorporation of PPMs into advanced polymer nanostructures has the potential to provide further enhancements in therapeutic activity while substantially reducing the cost and complexity of preparing multifunctional drug delivery systems.<sup>25,26</sup> To date a variety of sophisticated polymeric architectures have been prepared by RAFT polymerization methodology including stars, brushes, brushed-brushes, and bottlebrushes.<sup>27-29</sup> Hyperbranched polymers have also been investigated for drug delivery applications.<sup>30</sup> Hyperbranched polymers can be conveniently prepared by nitroxide-mediated polymerization (NMP)<sup>31</sup> and atom transfer radical polymerization (ATRP)<sup>32,33</sup> via the use of vinyl-functionalized initiators (inimers) or by RAFT using vinyl-functionalized CTAs (transmers).<sup>34-36</sup>

Hyperbranched polymers synthesized with inimers/transmers typically have larger molar mass dispersities; however, their constituent segments are still somewhat controlled. In this approach the degree of branching can be manipulated by simple adjustment of the inimer/transmer to monomer ratio and overall monomer conversion. For example, transmers have been employed to prepare architecturally distinct antigen carriers with pH-responsive endosomal-releasing segments.<sup>37</sup> In these studies, dendritically branched copolymers were synthesized using a methacrylate-functionalized RAFT CTA. Antigen delivery with the hyperbranched and cross-linked polymer architecture enhanced in vitro MHC-I antigen presentation relative to free antigen, whereas the linear construct did not have a discernible effect.

At present there have been few literature reports detailing the homopolymerization of transmers.<sup>30,38</sup> Homopolymerization of transmers using thermal initiators generally yield hyperbranched polymers with relatively low molecular weights.<sup>34,35,39</sup> In contrast, concurrent ATRP/RAFT polymerization of transmers have been shown to yield hyperbranched polymers over 500 kDa.<sup>40</sup> Unimolecular hyperstar polymer for siRNA delivery have also been synthesized by homopolymerization of ATRP inimers in microemulsion followed by solution polymerization of DMAEMA from the multifunctional core.<sup>41</sup> The resultant hyperstar-siRNA complexes showed in vitro transfection efficiencies higher than the Lipofectamine control. Herein we describe the development of mannose-targeted radiant star nanoparticle (RSN) prodrugs prepared by the copolymerization of PPMs with glycan monomers from homopolymerized transmer cores linked via ester or acetal bonds.

## B Experimental

### Materials

Chemicals and all materials were supplied by Sigma-Aldrich unless otherwise specified. 4-(((2-Carboxyethyl)thio)carbo-*no*thiyl)thio-4-cyanopentanoic acid (CCC) was kindly donated by Boron Molecular. Hydroxyethyl methacrylate (HEMA), and *N,N'*-dimethylacrylamide (DMA) were distilled under reduced pressure. Spectra/Por regenerated cellulose dialysis membranes (6-8 kDa cutoff) were obtained from Fisher Scientific.

4-Cyano-4-((ethylsulfanylthiocarbonyl)sulfanyl)pentanoic acid (ECT) was synthesized as described previously.<sup>42</sup> Sephadex G-25 prepacked PD10 columns were obtained from GE Life Sciences. 4-Cyano-4-ethylsulfanylthiocarbonylsulfanyl-4-methyl-butyrac acid 1-(2-methyl-acryloyloxy)-ethyl ester (hECT)<sup>37</sup>, mannose ethyl methacrylate (MEM)<sup>43</sup>, rhodamine B methacrylate (REMA)<sup>44</sup> and ciprofloxacin (tyramine) methacrylate (CTM)<sup>11</sup> were synthesized as described previously.

### Animal Ethics Statement

All animal work was conducted in accordance to the University of Washington's Institutional Animal Care and Use Committee, and Department of Defense's ACURO office guidelines. Experimental group sizes were approved by the regulatory authorities for animal welfare after being defined to balance statistical power, feasibility, and ethical aspects. All mice were kept in accordance with federal and state policies on animal research at the University of Washington.

**Synthesis of 4-Cyano-4-ethylsulfanylthiocarbonylsulfanyl-4-methyl-butyrac acid 2-{1-[2-(2-methyl-acryloyloxy)-ethoxy]-ethoxy}-ethyl ester (aECT).** To a 50 mL round bottom flask containing a magnetic stir bar was added ECT (5.0 g, 19.0 mmol, 1.0 equivalent), 4-dimethylaminopyridine (4.64 g, 38.0 mmol, 2 equivalents), *N,N'*-dicyclohexylcarbodiimide (4.7 g, 22.8 mmol, 1.2 equivalents), and 28 mL methylene chloride. To the solution was then added ethyleneglycol vinyl ether (4.01 g, 45.5 mmol, 2.4 equivalents). The round bottom flask was then capped with a rubber septa and allowed to react over ice for 1 hour and then at room temperature overnight. The solution was then filtered and then transferred to a separation funnel and was washed 5 times with saturated sodium bicarbonate solution. The organic phase was then collected, dried over anhydrous sodium sulfate, filtered through a plug of cotton, and then isolated via rotary evaporation. The product was then used for the synthesis of aECT without further purification (Yield 5.02 g, 70.0%). To a 10 mL round bottom flask was added EGVE-ECT (0.5 g, 1.5 mmol), HEMA (0.195 g, 1.5 mmol), TFA (50  $\mu$ L, 653  $\mu$ mol), and methylene chloride 1.0 mL. The reaction was then sealed with a septa and allowed to react overnight. The product was then isolated via silica gel column chromatography using an eluent consisting of ethyl acetate/hexanes (75:25) with 1 % triethylamine. <sup>1</sup>H NMR (500 MHz, benzene-d<sub>6</sub>, ppm)  $\delta$  = 6.16 (1H, singlet, vinyl), 5.24 (1H, vinyl), 4.52 (1H, quartet, acetal), 4.19 (2H, triplet, ester), 4.08

(2H, triplet, ester), 3.28-3.56 (4H, multiplet,  $\text{OCH}_2\text{CHCH}_3\text{OCH}_2$ ), 2.79 (2H, quartet,  $\text{SCH}_2$ ), 2.0-2.4 (4H, multiplet,  $\text{C}(\text{CH}_3)(\text{CN})\text{CH}_2\text{CH}_2$ ), 1.85 (3H, singlet, vinyl-methyl), 1.32 (3H, singlet,  $\text{C}(\text{CN})\text{CH}_3$ ), 1.13 (3H, doublet, acetal-methyl), and 0.82 (3H, triplet,  $\text{SCH}_2\text{CH}_3$ ) (for the labeled  $^1\text{H}$  NMR spectrum see supporting information).  $^{13}\text{C}$  NMR (125 MHz, benzene- $d_6$ , ppm)  $\delta$  = 216.9, 170.8, 136.6, 125.1, 118.7, 99.3, 63.9, 63.7, 62.6, 62.3, 33.8, 31.0, 29.5, 24.1, 19.2, 18.1, 12.2. (Yield 0.34 g, 48 %).

**Synthesis of poly(hECT) and poly(aECT).** To a 5 mL conical bottom flask was added either hECT (6.52 g, 17.36 mmol) or aECT (8.04 g, 17.36 mmol), ABCVA (486 mg, 1.76 mmol), and 15.2 mL of anhydrous DMSO. The flask was then sealed with a rubber septa and then purged with nitrogen for 30 minutes. The solution was then transferred to a preheated oil bath at 70 °C and allowed to polymerize for 18 h. The polymers were then isolated by precipitating the polymerization solution to 45 mL of diethyl ether in 50 mL conical tubes. After vortexing, the solutions were centrifuged at 4200 rpm for 5 minutes, the ether supernatant was decanted and yellow polymer oil was diluted 1 to 1 with acetone and reprecipitated into ether as described above (x6).

**Synthesis of DMA RSNs from poly(hECT) and poly(aECT).** Polymerization of DMA was conducted in DMSO in the presence of either poly(hECT) or poly(aECT) and ABCVA. The initial molar feed percentages of the Dt-SMA and O950 monomers were both 50 %. The  $[\text{M}]_0:[\text{CTA}]_0:[\text{I}]_0$  was 200:1:0.025 at an initial monomer concentration of 25 wt. %. To a 10 mL conical bottom flask was added poly(hECT) (20 mg, 53 mmol) or poly(aECT) (25 mg, 53 mmol), DMA (1.06 g, 10.7 mmol), ABCVA (0.373 mg, 1.3 mmol) and 3.17 mL DMSO. The polymerization solutions were then septa sealed and then purged with nitrogen for 30 minutes. After this time, the polymerization solution was transferred to a preheated oil bath at 70 °C and allowed to polymerize for 4 hours. The copolymer was isolated by precipitating the polymerization solution into 45 mL of diethyl ether in 50 mL conical tubes. After vortexing, the solutions were centrifuged at 4200 rpm for 5 minutes. The clear ether supernatant was decanted and yellow polymer oil was diluted 1 to 1 with acetone and reprecipitated into ether as described above (x6).

**Kinetic evaluation of the RAFT polymerization of DMA from poly(hECT).** The initial monomer ( $[\text{M}]_0$ ) to CTA equivalents to initiator ( $[\text{I}]_0$ ) ratio was 350:1:0.025 respectively. Individual polymerization solutions were transferred to a septa-sealed vial and purged with nitrogen for 30 minutes. After this time, the polymerization vials were transferred to a preheated oil bath at 90 °C and allowed to polymerize for the prescribed time period. In order to determine the monomer conversion 50  $\mu\text{L}$  of the polymerization solutions were first diluted into 900  $\mu\text{L}$  of  $\text{CDCl}_3$  and then  $^1\text{H}$  NMR spectra were recorded. The molar fraction of DMA converted to polymer was then determined by comparison of the total vinyl resonances (3H)

(A) between 5.0-6.5 ppm to the total backbone resonances between 0.5-1.5 ppm (B) using the equation: % DMA conversion =  $[(\text{A}+\text{B})-(\text{A})]/(\text{A}+\text{B}) \times 100$ .

**Synthesis of poly(mannose-co-CTM) RSN from poly(hECT).**

Copolymerization of MEM and CTM from poly(hECT) was conducted with an initial monomer  $[\text{M}]_0:[\text{CTA}]_0:[\text{I}]_0$  ratio was 100:1:0.05 at an initial overall monomer concentration of 20 % m/v. To a 5 mL conical bottom flask was added poly(hECT) (3.06 mg, 8.15  $\mu\text{mol}$ ), MEM (0.2 g, 0.684 mmol), CTM (0.1 g, 0.131 mmol), REMA (7.75 mg, 13.1  $\mu\text{mol}$ ), V70 (0.125 mg, 0.408  $\mu\text{mol}$ ) as 100  $\mu\text{L}$  of 1.25 mg  $\text{mL}^{-1}$  solution in dioxane, and 1.2 mL of DMSO. The polymerization solution was then septa-sealed purged with nitrogen for 30 minutes. After this time, the polymerization vials were transferred to a preheated oil bath at 30 °C and allowed to polymerize for 18 hours. After this time, the polymerization solution was precipitated into 45 mL of diethyl ether in 50 mL conical tubes. After vortexing, the solution was centrifuged at 4200 rpm for 5 minutes. The ether supernatant was decanted and yellow polymer oil was diluted to a final volume of 25 mL in 0.5 M phosphate buffer pH 7.4. The aqueous solution was dialyzed against deionized water at 5 °C using spectra/Por regenerated cellulose dialysis membranes (6-8 kDa cutoff) and isolated by lyophilisation. The lyophilized polymer was then redissolved in deionized water and then purified by double Sephadex G-25 prepacked PD10 columns according to the manufacturer's instructions.

**Synthesis of poly(DMA-co-CTM) RSN from poly(hECT).**

Copolymerization of DMA and CTM from poly(hECT) was conducted with an initial monomer  $[\text{M}]_0:[\text{CTA}]_0:[\text{I}]_0$  ratio was 100:1:0.05 at an initial overall monomer concentration of 20 % m/v. To a 5 mL conical bottom flask was added poly(hECT) (8.06 mg, 21.5  $\mu\text{mol}$ ), DMA (0.2 g, 2.02 mmol), CTM (0.1 g, 0.131 mmol), REMA (7.75 mg, 13.1  $\mu\text{mol}$ ), V70 (0.331 mg, 1.07  $\mu\text{mol}$ ) as 100  $\mu\text{L}$  of 3.31 mg  $\text{mL}^{-1}$  solution in dioxane, and 1.2 mL of DMSO. The polymerization solution was then septa-sealed and purged with nitrogen for 30 minutes. After this time, the polymerization vials were transferred to a preheated oil bath at 30 °C and allowed to polymerize for 18 hours. After this time, the polymerization solution was precipitated into 45 mL of diethyl ether in 50 mL conical tubes. After vortexing, the solution was centrifuged at 4200 rpm for 5 minutes. The ether supernatant was decanted and yellow polymer oil was diluted to a final volume of 25 mL in 0.5 M phosphate buffer pH 7.4. The aqueous solution was then dialyzed against deionized water at 5 °C using spectra/Por regenerated cellulose dialysis membranes (6-8 kDa cutoff) and then isolated by lyophilisation. The lyophilized polymer was then redissolved in deionized water and then purified by double Sephadex G-25 prepacked PD10 columns according to the manufacturer's instructions.

**Synthesis of linear poly(MEM-co-CTM).** Copolymerization of MEM and CTM in the presence of the trithiocarbonate-based RAFT agent CCC was conducted with an initial monomer  $[\text{M}]_0:[\text{CTA}]_0:[\text{I}]_0$  ratio was 100:1:0.05 at an initial overall

monomer concentration of 20 % m/v. To a 5 mL conical bottom flask was added CCC (2.50 mg, 8.15  $\mu\text{mol}$ ), MEM (0.2 g, 0.684 mmol), CTM (0.1 g, 0.131 mmol), REMA (7.75 mg, 13.1  $\mu\text{mol}$ ), V70 (0.125 mg, 0.408  $\mu\text{mol}$ ) as 100  $\mu\text{L}$  of 1.25 mg mL<sup>-1</sup> solution in dioxane, and 1.2 mL of DMSO. The polymerization solution was then septa-sealed and purged with nitrogen for 30 minutes. After this time, the polymerization vials were transferred to a preheated oil bath at 30 °C and allowed to polymerize for 18 hours. After this time, the polymerization solution was precipitated into 45 mL of diethyl ether in 50 mL conical tubes. After vortexing, the solution was centrifuged at 4200 rpm for 5 minutes. The ether supernatant was decanted and yellow polymer oil was diluted to a final volume of 25 mL in 0.5 M phosphate buffer pH 7.4. The aqueous solution was then dialyzed against deionized water at 5 °C using spectra/Por regenerated cellulose dialysis membranes (6-8 kDa cutoff) and then isolated by lyophilisation. The lyophilized polymer was then redissolved in deionized water and then purified by double Sephadex G-25 prepacked PD10 columns according to the manufacturer's instructions.

**Synthesis of linear poly(DMA-co-CTM).** Copolymerization of DMA and CTM in the presence of the trithiocarbonate-based RAFT agent CCC was conducted with an initial monomer [M]<sub>0</sub>: [CTA]<sub>0</sub>: [I]<sub>0</sub> ratio was 100:1:0.05 at an initial overall monomer concentration of 20 % m/v. To a 5 mL conical bottom flask was added CCC (6.60 mg, 21.5  $\mu\text{mol}$ ), DMA (0.2 g, 2.02 mmol), CTM (0.1 g, 0.131 mmol), REMA (7.75 mg, 13.1  $\mu\text{mol}$ ), V70 (0.331 mg, 1.07  $\mu\text{mol}$ ) as 100  $\mu\text{L}$  of 3.31 mg mL<sup>-1</sup> solution in dioxane, and 1.2 mL of DMSO. The polymerization solution was then septa-sealed and purged with nitrogen for 30 minutes. After this time, the polymerization vials were transferred to a preheated oil bath at 30 °C and allowed to polymerize for 18 hours. After this time, the polymerization solution was precipitated into 45 mL of diethyl ether in 50 mL conical tubes. After vortexing, the solution was centrifuged at 4200 rpm for 5 minutes. The ether supernatant was decanted and yellow polymer oil was diluted to a final volume of 25 mL in 0.5 M phosphate buffer pH 7.4. The aqueous solution was then dialyzed against deionized water at 5 °C using spectra/Por regenerated cellulose dialysis membranes (6-8 kDa cutoff) and then isolated by lyophilisation. The lyophilized polymer was then redissolved in deionized water and then purified by double Sephadex G-25 prepacked PD10 columns according to the manufacturer's instructions.

**Gel permeation chromatography (GPC).** Absolute molecular weights and polydispersity indices were determined using Tosoh SEC TSK-GEL  $\alpha$ -3000 and  $\alpha$ -e4000 columns (Tosoh Bioscience, Montgomeryville, PA) connected in series to an Agilent 1200 Series Liquid Chromatography System (Santa Clara, CA) and Wyatt Technology miniDAWN TREOS, 3 angle MALS light scattering instrument and Optilab TrEX, refractive index detector (Santa Barbara, CA). HPLC-grade DMF containing 0.1 wt.% LiBr at 60 °C was used as the mobile phase for p(hECT), p(aECT), and poly(DMA) at a flow rate of 1 mL/min. Copolymers containing mannose were evaluated in

an aqueous eluent consisting of 150 mM sodium acetate buffer at pH 4.4.

**Dynamic Light Scattering.** Particle sizes of the polymers were measured by dynamic light scattering (DLS) using a Malvern Zetasizer Nano ZS. Samples were prepared by dissolving lyophilized polymer in phosphate buffer saline (150 mM NaCl, 20 mM phosphates, pH 7.4), at a concentration of 1 mg mL<sup>-1</sup>.

**Transmission Electron Microscopy (TEM).** 0.5 mg mL<sup>-1</sup> samples were applied to glow-discharged continuous carbon film EM grids and negatively stained using 1% uranyl formate. Grids were imaged by transmission electron microscopy using an FEI Morgagni operating at 100 kV and a Gatan Orius Camera.

**Polymer hydrolysis studies.** The hydrolytic stability of poly(DMA) RSNs polymerized from p(hECT) and p(aECT) cores was evaluated at pH 4.8 and 7.4 in 150 mM acetate and phosphate buffer respectively. Polymers were dissolved in the buffers at a concentration of 25 mg mL<sup>-1</sup> and then incubated at 37 °C for the appropriate time period. Prior to analysis, a 200  $\mu\text{L}$  aliquot was diluted into 800  $\mu\text{L}$  of DMF. The sample was analyzed directly via gel permeation chromatography as described above.

**Analysis of ciprofloxacin by high-performance liquid chromatography (HPLC).** The HPLC analysis of ciprofloxacin was carried out with an Agilent 1260 Quaternary HPLC Pump, Agilent 1260 Infinity Standard Automatic Sampler, Agilent 1260 Infinity Programmable Absorbance Detector, and Agilent ChemStation software for LC system (Palo Alto, CA). Both ciprofloxacin hydrochloride and liquid Sera Human from AB blood donor were purchased from Sigma Aldrich and used as received. The analyte was separated at ambient temperature using a Zorbax RX-C18 (4.6  $\times$  150 mm; 5  $\mu\text{m}$ ) analytical column (Agilent Technologies, CA).

The UV detector was operated at 277 nm, and the mobile phase consisted of 2% aqueous acetic acid and acetonitrile (84:16) v/v, as described elsewhere. The flow rate was set at 1.0 mL min<sup>-1</sup> and sample injection volume at 20  $\mu\text{L}$ . A stock solution of ciprofloxacin was prepared in deionized water at 10 mg mL<sup>-1</sup>. Working solutions of ciprofloxacin for standard curves were diluted from stock solution using the mobile phase to the listed concentrations of 200  $\mu\text{g mL}^{-1}$ , 100  $\mu\text{g mL}^{-1}$ , 50  $\mu\text{g mL}^{-1}$ , 25  $\mu\text{g mL}^{-1}$ , 12.5  $\mu\text{g mL}^{-1}$ , 6.25  $\mu\text{g mL}^{-1}$ , 3.12  $\mu\text{g mL}^{-1}$ , and 1.56  $\mu\text{g mL}^{-1}$ . Each listed solution above was diluted with a 1:1 v/v ratio of either mobile phase:deionized water or mobile phase: human serum to create a final ciprofloxacin standards of 100  $\mu\text{g mL}^{-1}$ , 50  $\mu\text{g mL}^{-1}$ , 25  $\mu\text{g mL}^{-1}$ , 12.5  $\mu\text{g mL}^{-1}$ , 6.25  $\mu\text{g mL}^{-1}$ , 3.12  $\mu\text{g mL}^{-1}$ , 1.56  $\mu\text{g mL}^{-1}$ , and 0.78  $\mu\text{g mL}^{-1}$  for pharmaceutical and biological analysis, respectively. Both non-serum (mobile phase:deionized water) and serum standards were subsequently diluted to 50% (v/v) with acetonitrile to promote protein precipitation. Serum standards were centrifuged at 12 000g for 15 minutes and supernatants

were collected and filtered using a 0.45  $\mu\text{m}$  low protein binding filter before HPLC analysis. Non-serum standards were analyzed without the need for centrifugation. All standards were processed using a gradient HPLC elution profile, where the mobile phase transitioned to 100% acetonitrile over 15 minutes, followed by 10 minutes of column washing with acetonitrile and water and 5 minutes of equilibration with mobile phase.

**Drug release from polymeric prodrugs.** Drug release from polymeric prodrugs was carried out in human serum at 37 °C at a polymer concentration of 6 mg mL<sup>-1</sup>. Sample time points were collected on a regular basis. Quantification of total ciprofloxacin in the polymeric prodrugs was measured by taking 6 mg mL<sup>-1</sup> of polymer and dissolving it in 10% aq. H<sub>2</sub>SO<sub>4</sub> for 48 h at 25 °C. The HPLC with a gradient elution profile was used to quantify amount of drug released using the same instrument parameters set forth for drug standards. A 1:1 dilution of serum sample to 2% aqueous acetic acid and acetonitrile (84:16) v/v was conducted, followed by another 1:1 dilution with acetonitrile. The resulting samples were vortexed and centrifuged at 12 000g for 15 minutes. Supernatants were collected and filtered using a 0.45  $\mu\text{m}$  low protein-binding filter before running on the HPLC.

**In vitro uptake studies.** Experiments were conducted with MPI cells (passaged with 30 ng mL<sup>-1</sup> murine GM-CSF) seeded at 200,000 cells/well. The cells were treated with 20  $\mu\text{g mL}^{-1}$  of rhodamine labeled polymers (for 0.5 h, 2h, and 5h). To make sure equivalent fluorescence was dosed for all treatment groups, standard curves were calculated as a function of polymer concentration. At each time point, the cells were collected, washed, and resuspended with cold PBS containing 0.2% fetal bovine serum (FBS) to remove unbound polymer. All samples were kept on ice and uptake/association was detected using the Y1 channel (rhodamine B). Statistical analysis was performed by Student's paired t test. (\*) denotes a P-value of  $\leq 0.05$ . (\*\*) denotes a P-value of  $\leq 0.005$ . Error bars are reported as SDs. All samples were performed in triplicate unless noted otherwise.

**In vitro co-culture activity using a *B. thailandensis* infection model.** RAW 264.7 cells were seeded (700,000 cells/mL, 250  $\mu\text{L}$ /well) into a 48 well plate with antibiotic free DMEM containing 10% FBS, and incubated at 37°C with 5% CO<sub>2</sub>. After 18 hours, cells were infected with *F. novicida* U112 at early log phase of growth (OD<sub>600</sub>=0.2) at a multiplicity of infection of 50, and then incubated for 1 hour. Subsequently, growth media was replaced with fresh DMEM containing 10% FBS and 250  $\mu\text{g/mL}$  kanamycin to eliminate extracellular bacteria not internalized by the cells; cells were then incubated for another hour. Growth media was then replaced with fresh DMEM containing free ciprofloxacin or mannose-targeted RSN (equivalent to 1 or 10  $\mu\text{g/mL}$  ciprofloxacin). Cells were incubated for another 22 hours (24 hours post-infection). After incubation, cells were washed three times with 1x PBS and lysed with 100  $\mu\text{L}$  of PBS containing 0.1% [v/v] Triton X-100.

Lysates were serially diluted and plated onto triplicate TSB agar plates and incubated for 24 hours. CFUs were counted when individual bacterial colonies were distinguishable.

**Acute lung safety of ciprofloxacin delivery systems.** In order to determine the in vivo biocompatibility of the polymeric prodrugs after pulmonary administration, the lung toxicity profiles of endotracheally delivered poly(MEM-co-CTM) RSNs were evaluated using the metrics of animal weight change, tumor necrosis factor alpha (TNF- $\alpha$ ) concentration in lung tissue homogenate (LTH) and bronchoalveolar lavage fluid (BALF), and neutrophil infiltration into the lungs. The mice were anesthetized with 5% isoflurane for 5 min before administration of 50  $\mu\text{L}$  per mouse of PBS only (Corning 21-040-CV), or 20 mg/kg ciprofloxacin (n = 5) as polymer formulations in PBS, pH 7.4. All solutions were filtered (0.2  $\mu\text{m}$ ) and administered via endotracheal delivery using a Microsprayer® aerosolizer designed for use on mice (Penn-Century MSA-250-M, PA, USA). Mice were dosed as above once every 24 hours for three consecutive days. 24 hours after the final administration, mice were weighed, and then sacrificed by CO<sub>2</sub> asphyxiation and lavaged by cannulating tracheas with a 22G soft catheter (Exel International 14-841-10) prior to a 1 mL PBS flush and followed by three 0.8 mL flushes. Approximately 3 mL of lavage fluid was recovered per mouse. Lungs were removed, weighed, and placed into 1 mL PBS on ice. Lung tissues were mechanically homogenized with a Qiagen TissueRuptor (9001271) before addition of 1 mL of lysis buffer [PBS+1% Triton X-100 and 1 protease tablet/10 mL (Roche 1836153001)]. BALF was spun at 1,000 g for 15 min to pellet lavage cells. BAL cells were re-suspended into 0.5 mL RPMI 1640+10% FBS, mounted onto microscopy slides with a Cytospin centrifuge at 46 g for 5 min, and then stained with Hemacolor (EMD Millipore 65044) prior to cytology analysis. Stained slides were analyzed for macrophage to neutrophil ratios with a minimum of 200 cells counted per slide. Cell-free BALF and LTH TNF- $\alpha$  concentration was assayed using Biologend's paired TNF- $\alpha$  ELISA kit (430902).

## C Results and discussion

### Synthesis and characterization of transmers

In these studies we desired to develop hydrophilic single polymer nanoparticle prodrugs that combine both the favourable uptake and circulation properties of nanoparticle-based systems with the higher drug release rates often observed for molecularly soluble polymeric prodrugs. In order to achieve this objective, RAFT transmers were first homopolymerized to yield a hyperbranched polymer core containing multiple chain transfer agents (CTAs) from which linear polymeric prodrugs could then be grown using PPMs. As shown in Scheme 1, trithiocarbonate-based transmers containing cyanovaleric acid R-groups were employed in these studies because of the ability of these CTAs to effectively control the polymerization of methacrylate monomers while also allowing relatively high [CTA]<sub>0</sub>/[I]<sub>0</sub> ratios (e.g. 100:1) to be

employed. The latter consideration is important for minimizing star-star coupling during the second polymerization step. The transmers shown in Scheme 1 also contain a polymerizable methacrylate residue covalently bound to the CTA by either an alkyl ester or an acetal linkage. These linkages were hypothesized to yield hyperbranched cores that would degrade at different rates under aqueous conditions.

The alkyl ester-linked transmer (hECT) was prepared by conjugation of the RAFT agent ECT to HEMA via standard carbodiimide coupling chemistry using DMAP catalyst as described previously.<sup>37</sup> In order to synthesize the acetal-linked transmer (aECT) a two-step synthesis was employed where the CTA was first esterified with ethylene glycol vinyl ether, which was then reacted with HEMA in the presence of an acid catalyst to yield the desired product (See Supporting Information Fig. S1).

### Homopolymerization of transmers

Shown in Fig. 1a and 1b are the <sup>1</sup>H NMR spectra for the homopolymerized transmers with the resonances labelled. Notably the peaks have broadened considerably relative to the low molecular weight precursors with the disappearance of the vinyl resonances and the concurrent appearance of methylene and methyl resonances in the backbone region. GPC analysis of poly(hECT) and poly(aECT) (Fig. 2c and 2d) show molecular weight distributions that are unimodal and symmetric with molar mass dispersities around 1.30. The homo-polymerized transmers have relatively low molecular weights of 8700 Da and 9300 Da for the alkyl ester and acetal ester containing structures respectively. This corresponds to approximately 23 and 20 RAFT CTAs respectively per polymeric transmer core assuming a homogenous composition composed exclusively of the precursor transmers. This result is consistent with previous studies where a molecular weights of 8740 was observed for a homopolymerized transmer.<sup>34</sup>

### Polymerization from polymeric transmer cores

In order to prepare nanoparticle prodrugs from the homopolymerized transmer cores, we first investigated the RAFT polymerization of a range of methacrylate and acrylamide based monomers (Fig. 2). As can be seen in Fig. 2a and 2b, the RAFT polymerization of DMA from both transmer cores yields unimodal and symmetric molecular weight distributions that elute at much lower elution volumes. In these polymerizations a  $[M]_0/[CTA]_0/[I]_0$  ratio of 200:1:0.05 was targeted resulting in molecular weights and molar mass dispersities of 364 000/1.32 and 275 000/1.36 for the alkyl ester and acetal linked radiant star nanoparticles. The effect of  $[M]_0/[CTA]_0$  at a fixed  $[CTA]_0/[I]_0$  of 0.05 was next evaluated. As can be seen in Fig. 2c, a clean progression of molecular weights towards lower elution volumes is observed with increasing  $[M]_0/[CTA]_0$ , suggesting the ability to prepare RSNs with different molecular weights simply by controlling the initial reaction stoichiometry. In all cases the molecular weight

distributions remained symmetric and unimodal with moderate molar mass dispersities around 1.45. The ability to prepare methacrylate based RSNs was next evaluated by conducting RAFT polymerizations from the poly(hECT) core low molecular weight methacrylate monomers (HEMA and DMAEMA) and high molecular weight methacrylate monomers (PEGMA  $FW_{avg} \sim 300$  and 950). As shown in Fig. 2d-f, a higher degree of control was observed for the polymerization of the smaller methacrylate monomers DMAEMA and HEMA from the polymeric transmer core. Here relatively narrow and symmetric molecular weight distributions were observed with molecular weight and molar mass dispersities of 186 300/1.39 and 401 400/1.57 respectively. In contrast, the RAFT polymerization of the sterically bulky PEGMA monomers yielded somewhat asymmetric molecular weight distributions with the presence of a high molecular weight star-star coupling peak observed for both the O300 and O950 polymerizations. Nonetheless minimal low molecular weight contamination was observed in these polymerizations suggesting that the PEGMA based RSNs might still prove to be versatile nanoparticle prodrugs despite the presence of some heterogeneity.

### RSN morphology via Transmission Electron Microscopy (TEM) and hydrolytic stability.

Evaluation of the RSN morphology via TEM (Fig. 3a) shows that these structures seem to form somewhat irregular branchy structures that are consistent with the RSN morphology depicted in Scheme 2. Although aggregation of the RSNs was observed during TEM analysis, it is possible to identify individual particles that show hydrodynamic diameters that are consistent with the 24 nm determined via dynamic light scattering.

Next the hydrolytic stability of DMA-based RSNs derived from both the alkyl ester linked poly(hECT) and acetal poly(aECT) linked cores was evaluated. Acetals have been shown to hydrolyze rapidly under acidic conditions such as those found in the intracellular compartment of macrophages while polymeric alkyl ester remain more stable under these conditions.<sup>45</sup> Shown in Fig. 3b and 3c, are the GPC chromatograms for poly(DMA) polymerized from poly(hECT) and poly(aECT) cores. Here the polymers were incubated at 37 °C in 150 mM acetate buffer at pH 5.0 for the indicated time period before being diluted into DMF and analysed via GPC. As can be seen in Fig. 4a, an overlay of the molecular weight distributions for the alkyl ester linked RSN shows no visible change between the initial polymeric nanoparticle and those incubated in buffer for 30 days. In contrast, a progressive degradation of the high molecular weight peak is observed for the acetal linked RSN over the course of the 30 day incubation period. Here the relatively broad RSN peak is seen to reduce in area with the appearance of a narrow lower molecular species that is consistent with linear polymers liberated from the central core following acetal hydrolysis. The slower rate of acetal hydrolysis observed relative to low molecular weight

acetal species is hypothesized to arise from the hydrophobic environment of the central core.

### Synthesis of mannose-targeted RSN prodrugs

Therapeutic RSN prodrugs were next synthesized, as shown in Fig. 4, by copolymerizing the ciprofloxacin prodrug monomer (CTM) with a hydrophilic mannose monomer (MEM) from homopolymerized transmer cores containing either alkyl ester or acetal linkages. Phenyl ester linked prodrug polymerizable prodrug monomers were employed in these studies as we have shown previously that these species hydrolyze at significantly higher rates in human serum than the analogous alkyl ester analogue. Indeed we have recently observed high cure rates for mice treated with phenyl ester linked ciprofloxacin based polymeric prodrugs while alkyl ester linked derivatives as well as the free ciprofloxacin controls show no protection against the lethal mouse model of *Francisella tularensis* infection.<sup>21</sup> The mannose comonomer employed in these polymerizations functions as a biocompatible hydrophilic stabilizer while also efficiently targeting alveolar macrophages where many pathogens such as *Burkholderia pseudomallei* and *Francisella tularensis* are known to reside. Polymerizations were conducted with an initial mol fraction of CTM and MEM of 16 % and 84 % (33 wt. % CTM) with an  $[M]_0/[CTA]_0$  and  $[CTA]_0/[I]_0$  ratio of 100 and 0.05 respectively in DMSO. In order to suppress the reaction of the secondary amine present on ciprofloxacin with the polymeric chain transfer agents, polymerizations were conducted at 30 °C. In addition to these mannose based RSNs, materials containing DMA as the hydrophilic stabilizer as well as the analogous linear copolymers were also synthesized to serve as untargeted controls (vide infra).

Shown in Fig. 5a-d are the <sup>1</sup>H NMR spectra and molecular weight distributions for the poly(MEM-co-CTM) and poly(DMA-co-CTM) RSNs respectively. Resonances associated with residues from CTM as well as the respective MEM and DMA comonomers can be clearly observed in Fig. 5a and 5d respectively. Because of the complex nature of the poly(MEM-co-CTM) spectrum, copolymer composition was determined by acid hydrolysis followed by reverse phase HPLC analysis of the released ciprofloxacin relative to standard curves for both materials. Based on this analysis a molar copolymer composition of 20 % CTM / 80 % MEM and 19.7 % CTM / 80.3 % DMA was determined, which is in good agreement with the feed. These values yield RSN prodrugs with 40 wt. % CTM (17.5 % ciprofloxacin drug) and 39 wt. % CTM (17 % ciprofloxacin drug) respectively.

### Ciprofloxacin release studies

Shown in Fig. 6 is the percentage ciprofloxacin release as a function of time for polymeric prodrugs incubated in human serum. In this study the rate of antibiotic released via cleavage of the phenyl ester-linked drugs was evaluated as a function of polymer architecture and hydrophilic comonomer. Here the highest rates of ciprofloxacin release was observed for the

poly(DMA-co-CTM) and poly(MEM-co-CTM), where the amount of the hydrophobic prodrug monomer in the copolymer was limited to approximately 33 wt. % (feed). This composition has been observed to yield copolymers that are easily dispersed in phosphate buffer at concentrations as high as 200 mg/mL with sizes that are consistent with molecularly dissolved unimers. Comparable rates of drug release were observed for both the DMA and Man based copolymers where 50 % drug release was observed at 125 and 110 hours respectively. In contrast, ciprofloxacin release from poly(O950-b-CTM), where the hydrophobic prodrug residues are localized in a discrete block copolymer segment, was observed to be quite slow with less than 4 % drug release over the same time period. This result is consistent with our previous studies, where molecularly soluble copolymers of CTM and polyethylene glycol methyl ether methacrylate (FW ~ 950 Da) (O950) showed considerably higher hydrolysis rates than those observed for diblock copolymers where the hydrophobic prodrug monomer was localized in the interior of micelles under aqueous conditions at pH 7.4. Evaluation of the DMA and mannose based RSNs show hydrolysis rates that are slower than the linear copolymers at similar compositions but significantly faster than the hydrolysis rates observed for diblock copolymer micelles. For example, 31.4 % hydrolysis was observed for the DMA based RSN polymerized from a poly(hECT) transmer following 120 h incubation in human serum. This corresponds to 7.3 times more ciprofloxacin released than the poly(PEGMA-b-CTM) micelles and only 12.7 % less ciprofloxacin released than the linear copolymer. No dramatic difference in drug release rates were observed between RSN prodrugs prepared from alkyl ester and acetal cores. This result likely arises from the slow rate of RSN degradation relative to the time scale of the hydrolysis experiment and moderately low differences in ciprofloxacin release between the linear and RSN prodrugs. This finding also suggests that more hydrolytically unstable transmer linkages such as hemiacetal esters may provide further enhancements in drug release from RSNs.

### Macrophage binding studies and in vitro co-culture activity using a *B. thailandensis* infection model

Previously, we have shown that primary and immortalized macrophages show distinct differences in mannose receptor expression levels with the primary cells showing significantly higher levels of the receptor. In order to evaluate the ability of the RSN prodrugs to target the macrophage mannose receptor, self-renewing, non-transformed MPI cells were first treated with 30 ng/mL murine GM-CSF to induce macrophage differentiation. Functionally, these cells have been known to closely resemble alveolar macrophages more so than immortalized cell-lines.<sup>46</sup> The cells were then treated with rhodamine B labelled poly(MEM-co-CTM) and poly(DMA-co-CTM) RSNs as well as the analogous linear controls for 30, 60, and 120 minutes. To make sure equivalent fluorescence was dosed for all treatment groups, standard curves were produced as a function of polymer concentration. Flow

cytometry was then employed to evaluate the amount of fluorescence for each treatment group. As shown in Fig. 7 (a), cells treated for 30 minutes show an initial but modest increase in fluorescence for both the linear and RSN containing mannose-targeting groups (444 and 2037 respectively) while the untargeted materials show low fluorescence close to untreated controls. Evaluation of the histograms following 120 minutes of treatment (7b) shows a significant increase in fluorescence for mannose-targeted RSN compared to the remaining treatment groups. These differences were observed to be the most apparent at 300 minutes (7c) where the mannose targeted RSN prodrugs showed approximately 6 times the fluorescence as the other treatment groups. These results, which are plotted in Fig. 7d, suggest that the combination of mannose targeting groups with nanoparticle dimensions provide substantially enhanced macrophage binding relative to both mannose targeted linear copolymers and untargeted RSNs.

The ability of the Mannose-targeted RSNs to effectively release ciprofloxacin in an active form within intracellular compartments was evaluated using a co-cultured model of *B. thailandensis*. In these studies a near quantitative elimination of colony forming units was observed at a polymeric ciprofloxacin concentration of  $10 \mu\text{g mL}^{-1}$  (CFUs =  $73 \pm 61$ ) while at a concentration of  $1.0 \mu\text{g mL}^{-1}$  bacteria levels were similar to negative controls with CFUs of  $300,000 \pm 4,6,900$  and  $39,000 \pm 1,6,800$ . While free ciprofloxacin showed complete antibiotic activity at a concentration of  $1.0 \mu\text{g mL}^{-1}$  we have observed previously that it is eliminated rapidly from circulation ( $k_{el}$  of  $0.7 \text{ h}^{-1}$ ) and shows negligible in vivo activity while the polymeric prodrugs with phenyl ester linked ciprofloxacin have higher retention times and show high cure rates. Given the higher rate of macrophage binding observed via flow cytometry for mannose-targeted RSNs relative to the linear copolymers we believe that their in vivo activity could be superior despite showing slightly lower drug release kinetics. It should be noted that in vitro cytotoxicity studies conducted in these cells showed no differences in cell viability relative to negative controls (See Supplementary Information Fig. S3).

#### In vivo biocompatibility of RSN prodrugs

In order to determine the in vivo biocompatibility of the RSN prodrugs following pulmonary administration, the lung toxicity of endotracheally delivered poly(MEM-co-CTM) prepared from a poly(hECT) transmer core was evaluated using the metrics of animal weight change (Fig. 7e), and neutrophil infiltration into the lungs (Fig. 7f), tumor necrosis factor alpha (TNF- $\alpha$ ) concentration in lung tissue homogenate (LTH) (Fig. 7g), and bronchoalveolar lavage fluid (BALF) (Fig. 7h). Here mice were dosed with the RSN at 20 mg/kg ciprofloxacin once every 24 h for three-consecutive days. These data demonstrate no statistical differences ( $P \leq 0.1$ ) across all observed toxicity markers at either drug dose for the poly(MEM-co-CTM) RSN prodrug compared to PBS controls. As shown in Fig. 7 (d-g), three consecutive doses resulted in lavage fluids containing  $5.7 \pm 1.8 \%$  neutrophils, respectively, whereas PBS controls

exhibited  $3.7 \pm 7.0 \%$  neutrophils. Similarly, TNF- $\alpha$  concentrations in both the LTH and BALF remained low and comparable to PBS control administrations.

## Conclusions

Homopolymerization of alkyl ester and acetal linked transmers yielded hyperbranched polymer cores with relatively low molecular weights and unimodal molecular weight distributions. Subsequent RAFT copolymerizations from the hyperbranched transmer cores enabled the synthesis of RSNs with high molecular weights, symmetric molecular weight distributions, and low amounts of homopolymer impurity. Hydrolysis studies conducted in acetate buffer from the alkyl ester and acetal linked cores demonstrated the high aqueous stability of the former while the latter showed a progressive degradation into unimeric species over the same period. Drug release studies conducted directly in 100 % human serum showed that the RSN prodrugs provided a substantial increase in ciprofloxacin release relative to diblock copolymer micelles with only a modest reduction in release relative to linear copolymer controls. Flow cytometry studies conducted in RAW264.7 cells induced to express the mannose receptor show significantly higher levels of cell binding for mannose-targeted RSN prodrugs relative to untargeted RSNs as well as both targeted and untargeted linear control polymers. In vivo biocompatibility studies showed no statistical differences between mice treated with mannose-targeted RSNs and phosphate buffer negative control mice. These results taken together suggest that RSNs provide a promising and simple strategy for preparing biocompatible nanoparticle prodrugs with enhanced drug release and receptor binding properties.

## Conflicts of interest

There are no conflicts to declare.

## Acknowledgements

This work was funded by the Defense Threat Reduction Agency (Grant #HDTRA1-13-1-0047).

## Notes and references

- 1 T. M. Allen and P. R. Cullis, *Advanced Drug Delivery Reviews*, 2013, **65**, 36–48.
- 2 S. Eliasof, D. Lazarus, C. G. Peters, R. I. Case, R. O. Cole, J. Hwang, T. Schlupe, J. Chao, J. Lin, Y. Yen, H. Han, D. T. Wiley, J. E. Zuckerman and M. E. Davis, *PNAS*, 2013, **110**, 15127–15132.
- 3 J. Cheng, K. T. Khin, G. S. Jensen, A. Liu and M. E. Davis, *Bioconjugate Chemistry*, 2003, **14**, 1007–1017.
- 4 H. Han and M. E. Davis, *Mol. Pharm.*, 2013, **10**, 2558–2567.
- 5 K. Cho, X. Wang, S. Nie, Z. G. Chen and D. M. Shin, *Clin Cancer Res*, 2008, **14**, 1310–1316.

- 6 M. E. Davis, Z. G. Chen and D. M. Shin, *Nat Rev Drug Discov*, 2008, **7**, 771–782.
- 7 R. K. Jain and T. Stylianopoulos, *Nat Rev Clin Oncol*, 2010, **7**, 653–664.
- 8 J. A. Alfurhood, H. Sun, C. P. Kabb, B. S. Tucker, J. H. Matthews, H. Luesch and B. S. Sumerlin, *Polym. Chem.*, 2017, **41**, 2545.
- 9 M. B. L. Kryger, A. A. A. Smith, B. M. Wohl and A. N. Zelikin, *Macromolecular Bioscience*, 2014, **14**, 173–185.
- 10 M. B. L. Kryger, B. M. Wohl, A. A. A. Smith and A. N. Zelikin, *Chemical Communications*, 2013, **49**, 2643–2645.
- 11 D. Das, S. Srinivasan, A. M. Kelly, D. Y. Chiu, B. K. Daugherty, D. M. Ratner, P. S. Stayton and A. J. Convertine, *Polymer Chemistry*, 2016, **7**, 826–837.
- 12 M. C. Parrott, M. Finniss, J. C. Luft, A. Pandya, A. Gullapalli, M. E. Napier and J. M. DeSimone, *JACS*, 2012, **134**, 7978–7982.
- 13 H. N. Son, S. Srinivasan, J. Y. Yhee, D. Das, B. K. Daugherty, G. Y. Berguig, V. G. Oehle, S. H. Kim, K. Kim, I. C. Kwon, P. S. Stayton and A. J. Convertine, *Polymer Chemistry*, 2016, 4494–4505.
- 14 D. Das, D. Gerboth, A. Postma, S. Srinivasan, H. Kern, J. Chen, D. M. Ratner, P. S. Stayton and A. J. Convertine, *Polymer Chemistry*, 2016, **7**, 6133–6143.
- 15 F. Joubert, L. Martin, S. Perrier and G. Pasparakis, *Macro Letters*, 2017, **6**, 535–540.
- 16 J. Sun, Y. Liu, Y. Chen, W. Zhao, Q. Zhai, S. Rathod, Y. Huang, S. Tang, Y. T. Kwon, C. Fernandez, R. Venkataramanan and S. Li, *Journal of Controlled Release*, 2017, **258**, 43–55.
- 17 M. Danial, S. Telwate, D. Tyssen, S. Cosson, G. Tachedjian, G. Moad and A. Postma, *Polym. Chem.*, 2016, **7**, 7477–7487.
- 18 Z. Duan, Y. Zhang, H. Zhu, L. Sun, H. Cai, B. Li, Q. Gong, Z. Gu and K. Luo, *ACS Appl Mater Interfaces*, 2017, **9**, 3474–3486.
- 19 H. B. Kern, S. Srinivasan, A. J. Convertine, D. Hockenbery, O. W. Press and P. S. Stayton, *Mol. Pharm.*, 2017, **14**, 1450–1459.
- 20 U. Hasegawa, A. J. van der Vlies, C. Wandrey and J. A. Hubbell, *Biomacromolecules*, 2013, **14**, 3314–3320.
- 21 D. Das, J. Chen, S. Srinivasan, A. M. Kelly, B. Lee, H.-N. Son, F. Radella, T. E. West, D. M. Ratner, A. J. Convertine, S. J. Skerrett and P. S. Stayton, *Mol. Pharm.*, 2017, **14**, 1988–1997.
- 22 R. Duncan, *Nat Rev Drug Discov*, 2003, **2**, 347–360.
- 23 S. Kim, Y. Shi, J. Y. Kim, K. Park and J.-X. Cheng, *Expert Opin Drug Deliv*, 2010, **7**, 49–62.
- 24 A. Vonarbourg, C. Passirani, P. Saulnier and J. P. Benoit, *Biomaterials*, 2006, **27**, 4356–4373.
- 25 C. E. Wang, P. S. Stayton, S. H. Pun and A. J. Convertine, *Journal of Controlled Release*, 2015.
- 26 T. Sun, Y. S. Zhang, B. Pang, D. C. Hyun, M. Yang and Y. Xia, *Angewandte Chemie International Edition in English*, 2014, **53**, 12320–12364.
- 27 C. J. Hawker, *Angewandte Chemie International Edition in English*, 1995, **34**, 1456–1459.
- 28 T.-H. Tran, C. T. Nguyen, L. Gonzalez-Fajardo, D. Hargrove, D. Song, P. Deshmukh, L. Mahajan, D. Ndaya, L. Lai, R. M. Kasi and X. Lu, *Biomacromolecules*, 2014, **15**, 4363–4375.
- 29 D. D. Lane, D. Y. Chiu, F. Y. Su, S. Srinivasan, H. B. Kern, O. W. Press, P. S. Stayton and A. J. Convertine, *Polym. Chem.*, 2014.
- 30 X. Wang and H. Gao, *Polymers*, 2017, **9**, 188.
- 31 C. J. HAWKER, J. Fréchet, R. B. GRUBBS and J. DAO, *J. Am. Chem. Soc.*, 1995, **117**, 10763–10764.
- 32 S. G. Gaynor, S. Edelman and K. Matyjaszewski, *Macromolecules*, 1996, **29**, 1079–1081.
- 33 S. K. Misra, X. Wang, I. Srivastava, M. K. Imgruet, R. W. Graff, A. Ohoka, T. L. Kampert, H. Gao and D. Pan, *Chem. Commun. (Camb.)*, 2015, **51**, 16710–16713.
- 34 A. P. Vogt and B. S. Sumerlin, *Macromolecules*, 2008.
- 35 J. Schmitt, N. Blanchard and J. Poly, *Polym. Chem.*, 2011, **2**, 2231–2238.
- 36 C. Zhang, Y. Zhou, Q. Liu, S. Li, S. Perrier and Y. Zhao, *Macromolecules*, 2011, **44**, 2034–2049.
- 37 J. T. Wilson, A. Postma, S. KELLER, A. J. Convertine, G. Moad, E. Rizzardo, L. Meagher, J. Chiefari and P. S. Stayton, *AAPS J*, 2015, **17**, 358–369.
- 38 M. Zhang, H. Liu, W. Shao, C. Ye and Y. Zhao, *Macromolecules*, 2012, **45**, 9312–9325.
- 39 Z. Wang, J. He, Y. Tao, L. Yang, H. Jiang and Y. Yang, *Macromolecules*, 2003, **36**, 7446–7452.
- 40 X. Wang, Y. Shi, R. W. Graff, X. Cao and H. Gao, *Macromolecules*, 2016, **49**, 6471–6479.
- 41 L. Zhao, X. Wu, X. Wang, C. Duan, H. Wang, A. Punjabi, Y. Zhao, Y. Zhang, Z. Xu, H. Gao and G. Han, *Macro Letters*, 2017, **6**, 700–704.
- 42 A. J. Convertine, D. S. W. Benoit, C. L. Duvall, A. S. Hoffman and P. S. Stayton, *J Control Release*, 2009, **133**, 221–229.
- 43 E.-H. Song, M. J. Manganiello, Y.-H. Chow, B. Ghosn, A. J. Convertine, P. S. Stayton, L. M. Schnapp and D. M. Ratner, *Biomaterials*, 2012, **33**, 6889–6897.
- 44 J. Chen, H.-N. Son, J. J. Hill, S. Srinivasan, F.-Y. Su, P. S. Stayton, A. J. Convertine and D. M. Ratner, *Nanomedicine: Nanotechnology, Biology and Medicine*, 2016, **12**, 2031–2041.
- 45 E. R. Gillies, A. P. Goodwin and J. Fréchet, *Bioconjugate chemistry*, 2004.
- 46 G. Fejer, M. D. Wegner, I. Gyoery, I. Cohen, P. Engelhard, E. Voronov, T. Manke, Z. Ruzsics, L. Doelken, O. P. da Costah, N. Branzk, M. Huber, A. Prasse, R. Schneider, R. N. Apte, C. Galanos and M. A. Freudenberg, *Proc. Natl. Acad. Sci. U.S.A.*, 2013, **110**, E2191–E2198.

Scheme 1. Overall synthetic strategy for the synthesis of radiant star nanoparticle (RSN) and starburst nanoparticle (SBN) prodrugs via RAFT polymerization from homopolymerized transmer cores.

Fig 1. <sup>1</sup>H NMR spectra and molecular weight distributions for the poly(hECT) and poly(aECT) hyperbranched transmer cores synthesized via homopolymerization of hECT and aECT.

Fig. 2a-g Molecular weight distributions for polymeric transmer cores as well as the corresponding RSN for (a) dimethyl acrylamide (DMA) from p(hECT), (b) DMA from p(aECT), (c) DMA from p(hECT) targeting multiple degrees of polymerization (d) N,N-dimethylaminoethyl methacrylate (DMAEMA), (e) 2-hydroxyethyl methacrylate (HEMA), (f) polyethyleneglycol monomethyl ether methacrylate (FW~300 Da) (O300) and (g) polyethyleneglycol monomethyl ether methacrylate (FW~950 Da) (O950). Molecular weight, molar mass dispersity ( $\bar{M}_w/\bar{M}_n$ ), and % monomer conversion values were determined to be: (poly(hECT) 8700:1.42:99.9, poly(aECT) 9300:1.43:99.9, DMA (DP200) poly(hECT) 364,000:1.32:85%, DMA poly(aECT) (DP200) 275 000:1.36:79%, DMAEMA (DP150) 186 300:1.39:48%, HEMA(DP150) 401 400:1.57:63%, O300 (DP80) 924,000:3.40:79%, O950 (DP25) 417,600:2.30:71%.

Fig. 3 (a) TEM analysis of poly(mono-2-(Methacryloyloxy)ethyl succinate) radiant star nanoparticles prepared from poly(hECT) core targeting a DP of 200. Molecular weight distributions for poly(DMA) polymerized from poly(hECT) (b) and poly(aECT) (c) transmer cores following incubation in pH 5.0 acetate buffer at 37 °C.

Fig 4. Synthetic scheme for the preparation of mannose targeted RSNs prodrugs via direct RAFT copolymerization of glycan functionalized monomer (Man) with the phenyl ester linked ciprofloxacin monomer (CTM) from polymeric transmer cores. Schematic illustration showing the mannose targeted RSN prodrug being internalized by alveolar macrophages following binding to the mannose receptor.

Fig. 5 <sup>1</sup>H NMR spectra in D<sub>6</sub> DMSO for poly(MEM-co-CTM) (a) and poly(DMA-co-CTM) (b) as well as the corresponding molecular weight distributions (c,d). Molecular weight, molar mass dispersity ( $\bar{M}_w/\bar{M}_n$ ) values were determined to be 490,000/1.38 and 452,000/1.43 respectively.

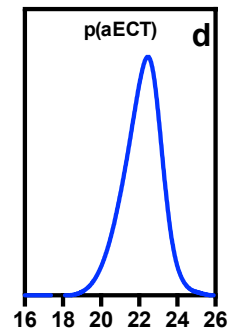
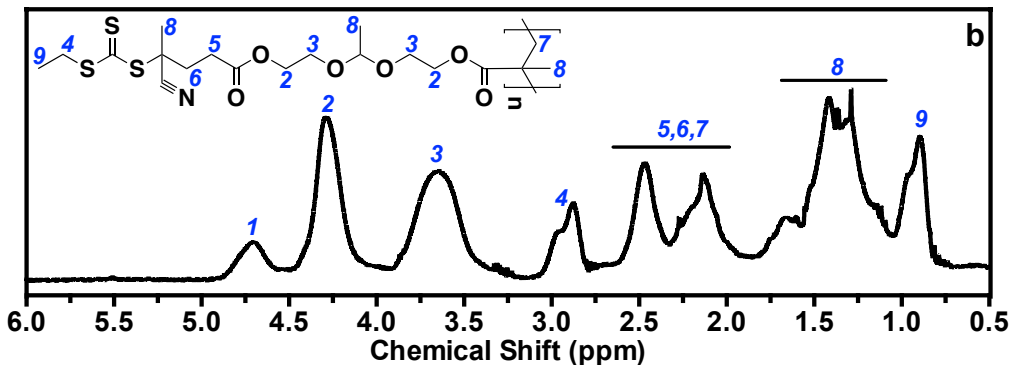
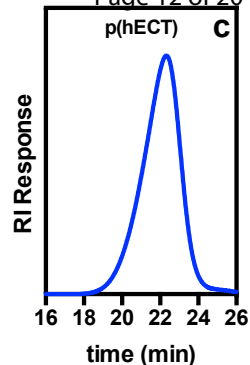
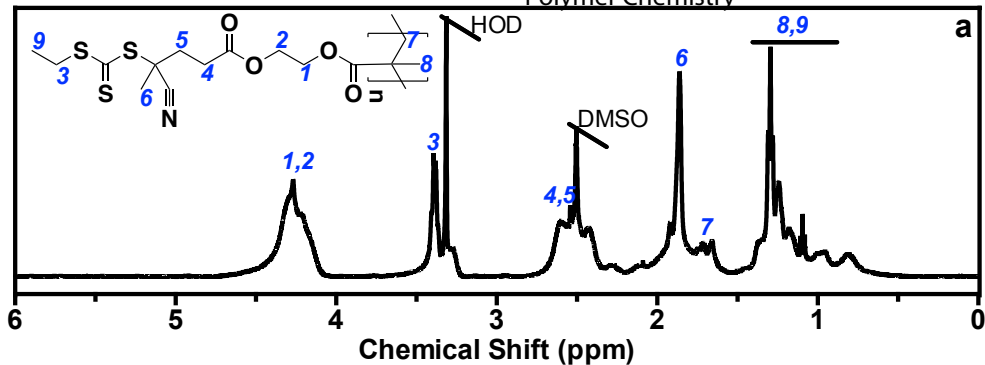
Fig. 6 Ciprofloxacin release from polymers incubated in 100 % human serum at 37 °C. Radiant star nanoparticles containing CTM copolymerized with DMA (open circles) show significantly faster ciprofloxacin release kinetic relative to diblock copolymer micelles with CTM core segments (solid black circles) but somewhat slower than soluble copolymers with DMA and Mannose (solid red and blue circles).

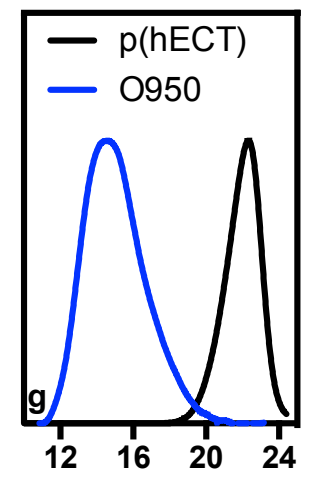
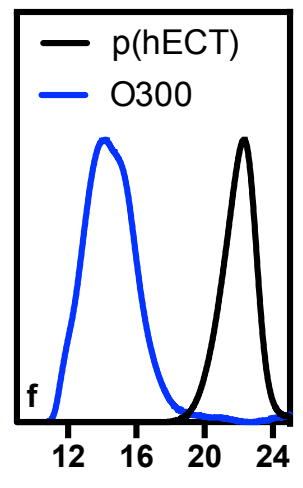
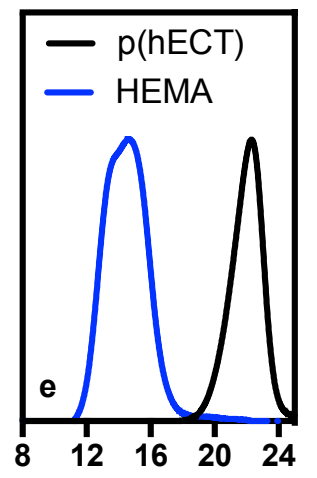
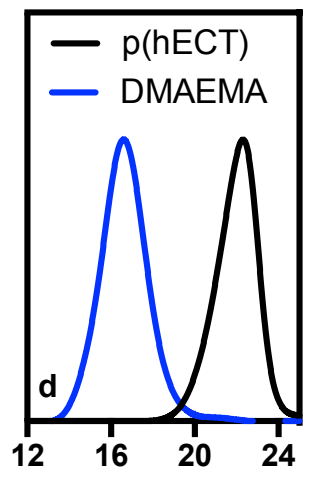
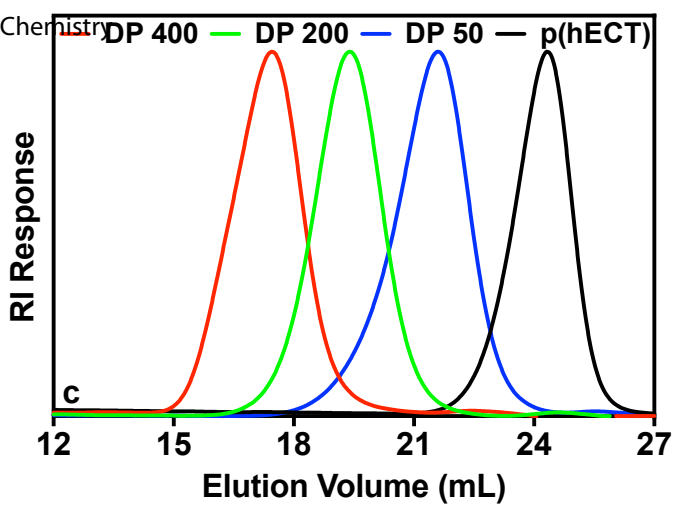
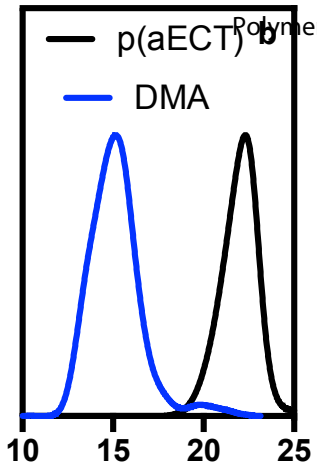
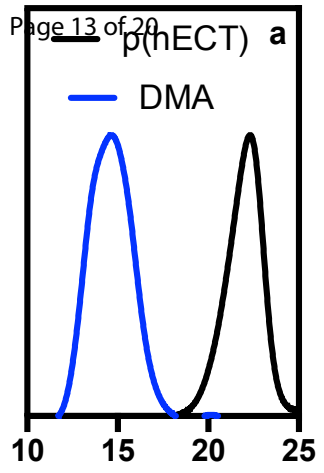
Fig. 7 (a-d) Flow cytometry studies conducted in IL4 transformed RAW264.7 cells comparing the cell binding properties of mannose-targeted and untargeted RSN

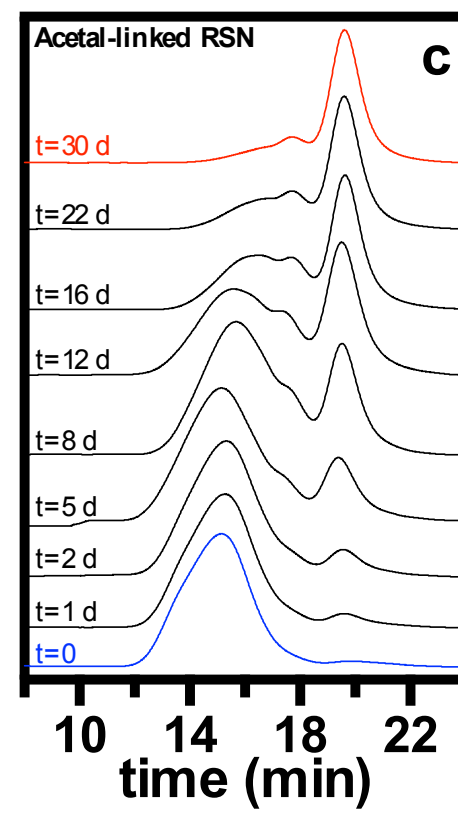
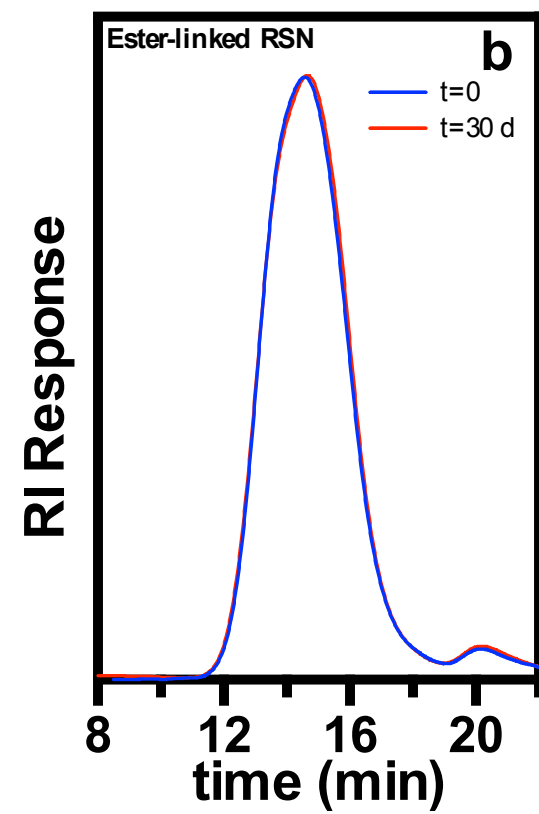
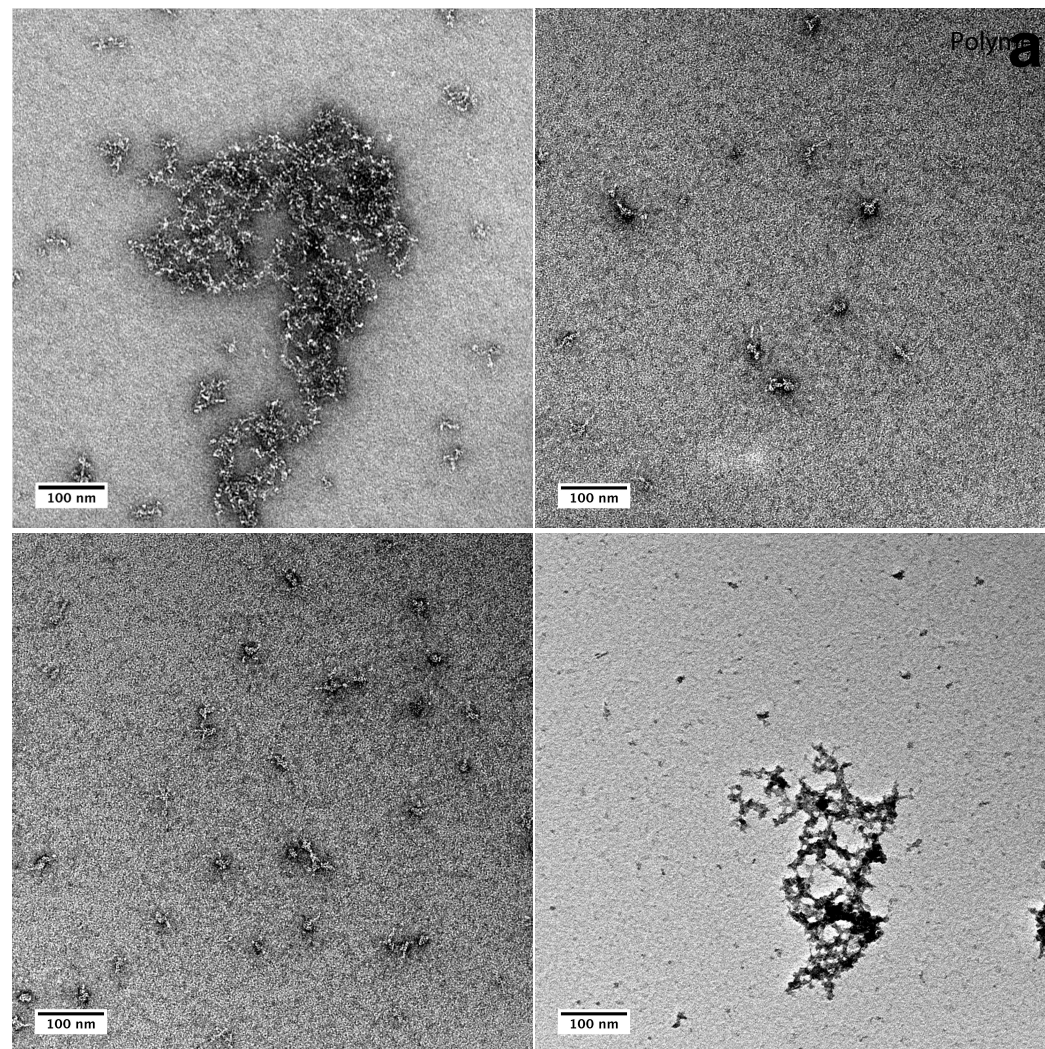
prodrugs as well as the linear controls. (e-h) Pulmonary toxicity of endotracheally delivered poly(Man-co-CTM) RSN prodrugs dosed at 20 mg/kg ciprofloxacin every 24 h over three- consecutive days.

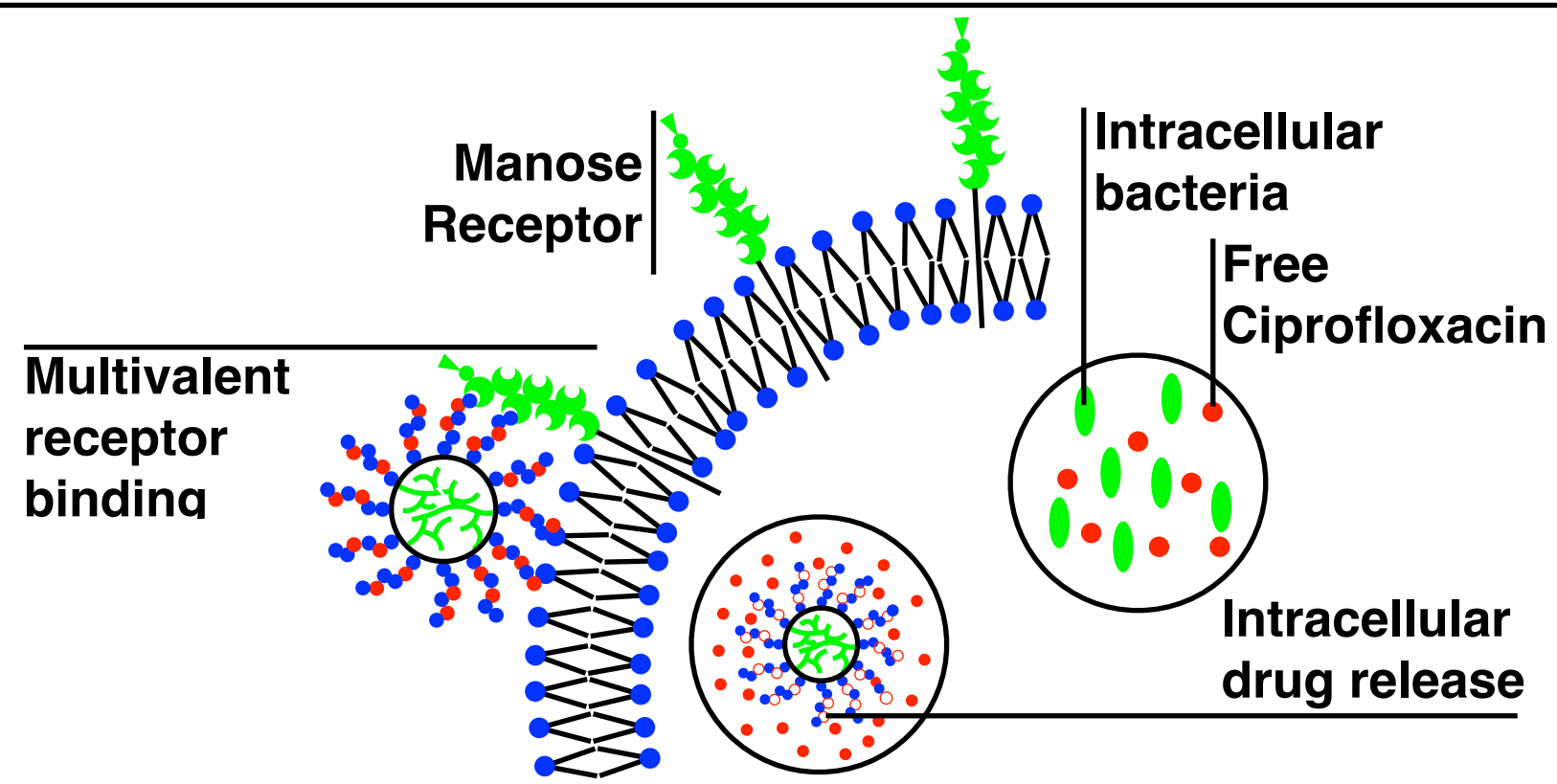
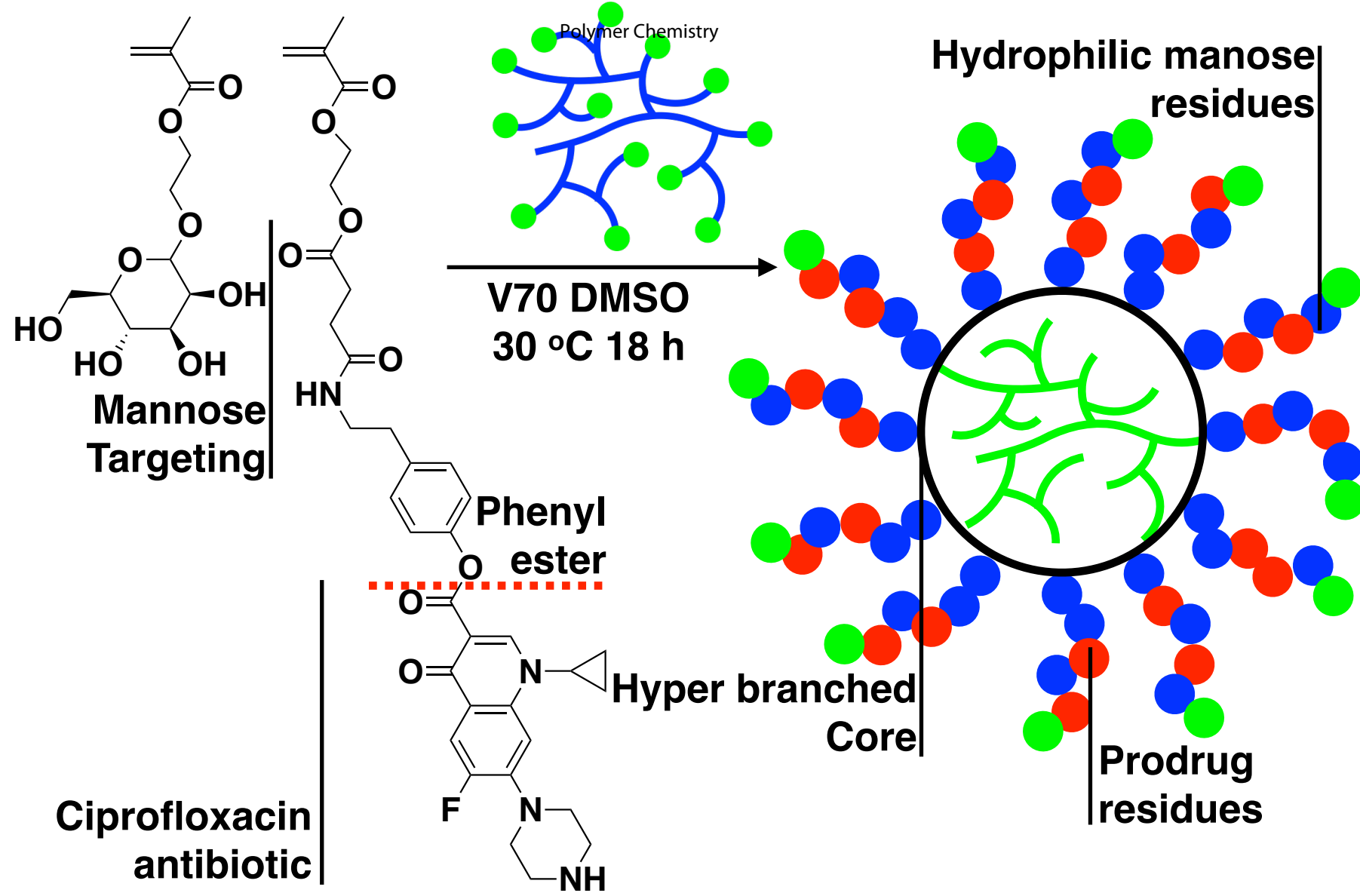
#### Table of Contents Text

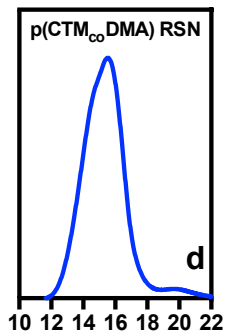
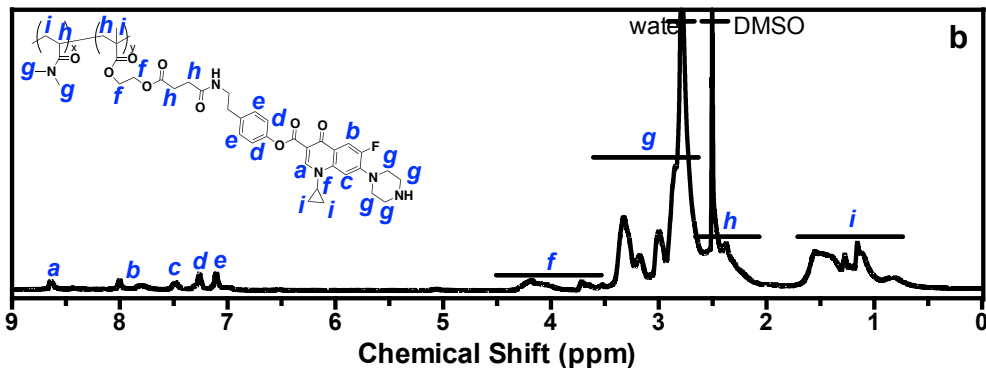
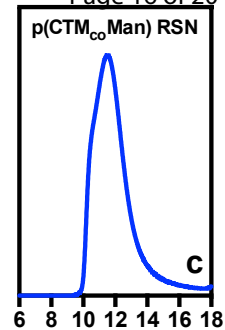
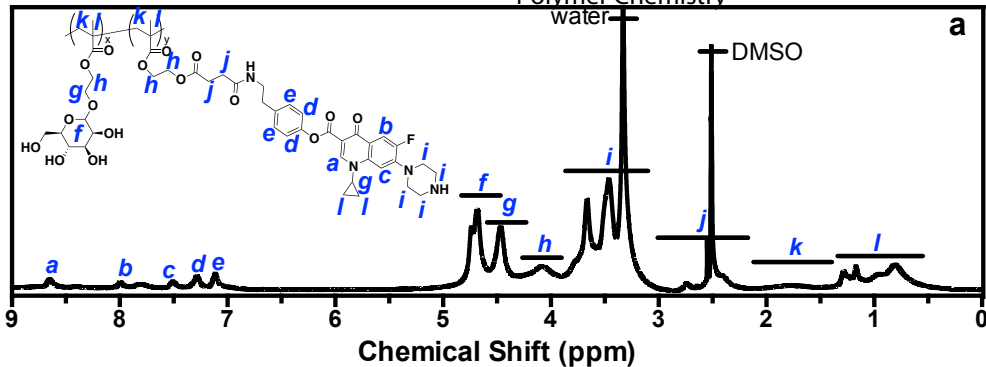
Radiant star nanoparticle prodrugs were synthesized in a two-step process by first homopolymerizing RAFT transmers followed by copolymerization from the hyperbranched polymer core.



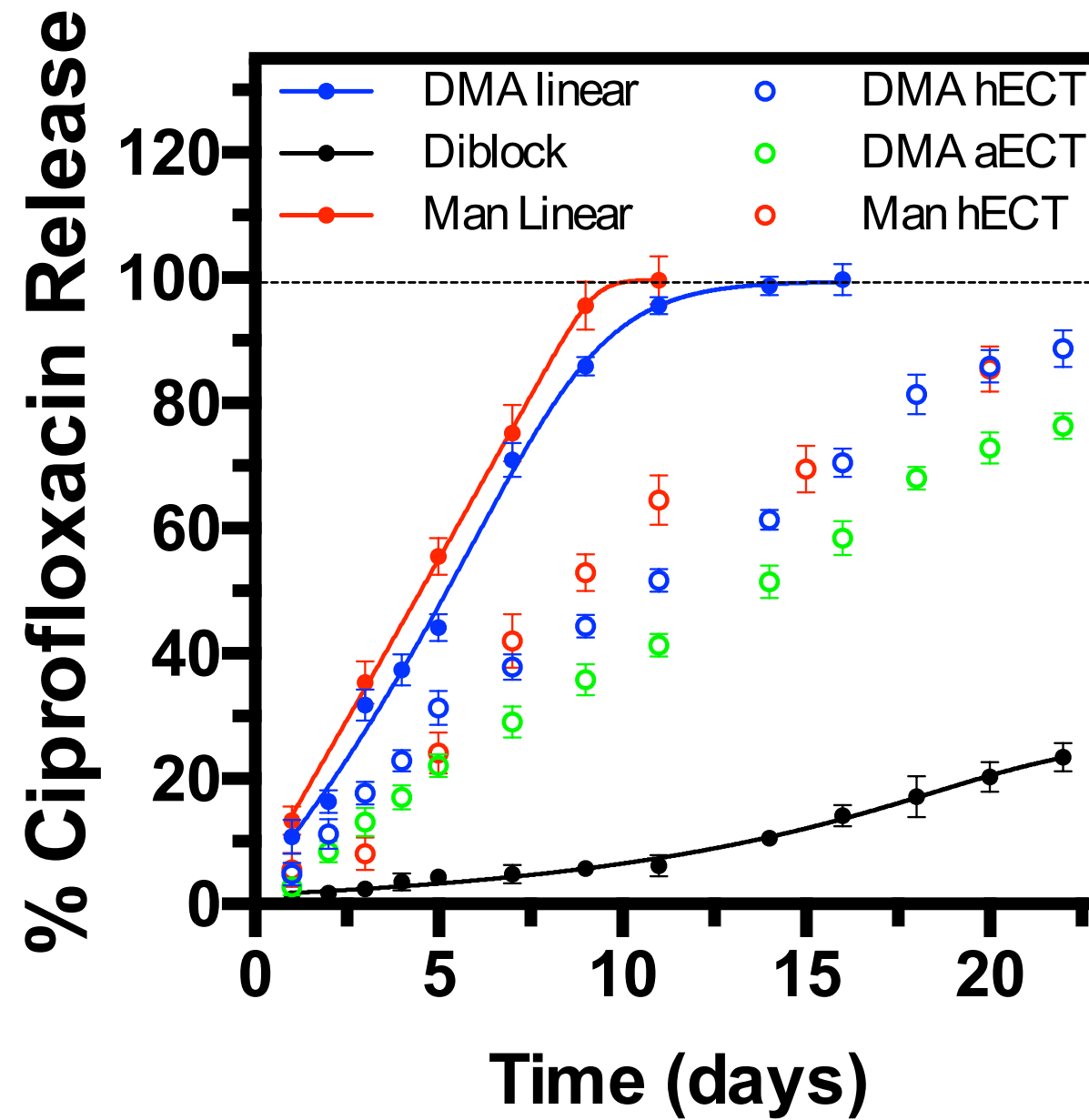


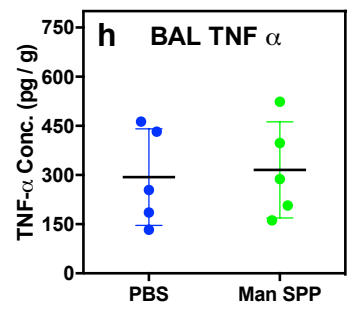
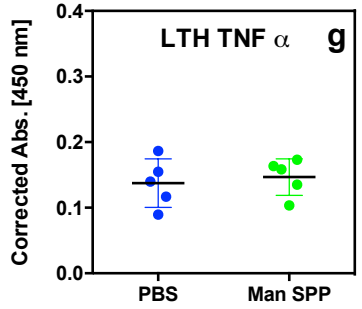
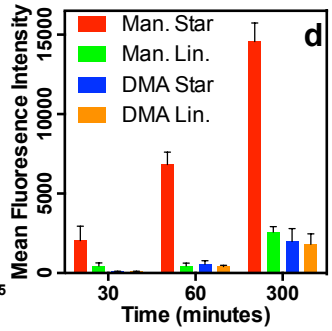
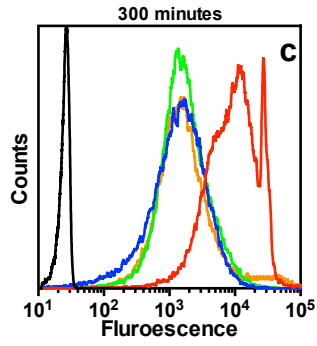
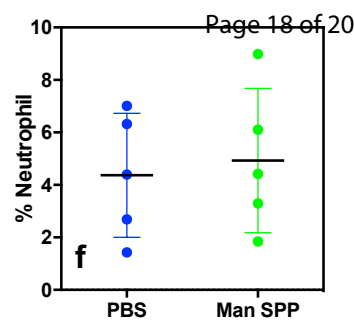
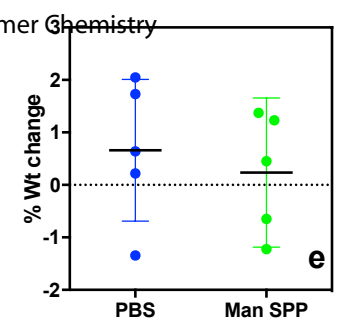
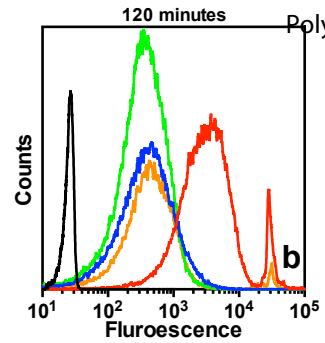
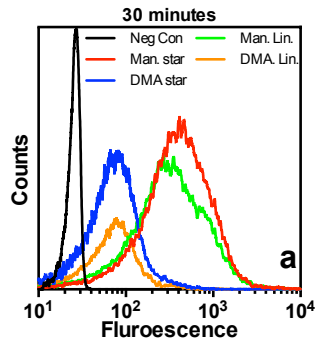




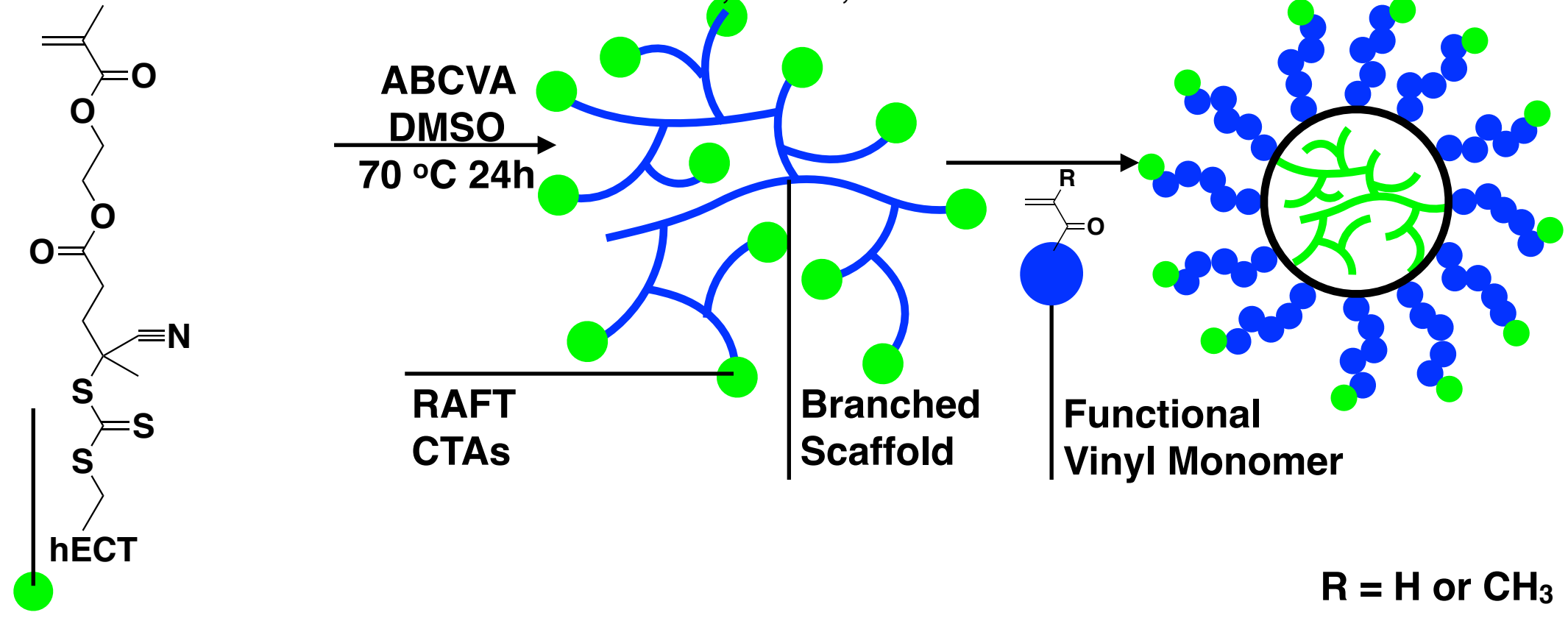


- DMA<sub>co</sub>CTM copolymer    DMA (ester) RSN ○
- Man<sub>co</sub>CTM copolymer    DMA (acetal) RSN ○
- PEGMA<sub>block</sub>CTM micelle    Man (ester) RSN ○





### a. Synthesis of radiant star nanoparticles



### b. Synthesis of pH-sensitive starburst nanoparticles

